Secondary Reactions in the High-Temperature Free Radical Polymerization of Butyl Acrylate

Adam N. F. Peck and Robin A. Hutchinson*

Department of Chemical Engineering, Dupuis Hall, Queen's University, Kingston, Ontario K7L 3N6, Canada

Received February 25, 2004; Revised Manuscript Received May 27, 2004

ABSTRACT: Secondary reactions have a marked effect on butyl acrylate polymerization rate and polymer structure under the high-temperature free radical reaction conditions typically used for production of solvent-based acrylic coatings resins. The low monomer concentrations characteristic of semibatch starved-feed reactor operation lead to significant rates of intramolecular transfer, resulting in a tertiary radical center capable of termination, monomer addition, or β-scission. The rate coefficients for these reactions are estimated from monomer concentrations, polymer molecular weights, and NMR analyses of quaternary branch points and macromer end groups for a series of semibatch experiments with varying monomer and polymer concentrations. A classical free radical polymerization model is insufficient for the description of this complex system. Thus, a mechanistic model including the additional reactions has been formulated and is shown to provide a good representation of the experimental results.

Introduction

Environmental restrictions and regulations play an increasing role in governing the production of acrylic coatings used for automotive markets. To accommodate the environmental goal of low solvent, high solid automotive coatings, base acrylic resins now consist of low molecular weight (MW) functionalized polymer produced via semibatch solution polymerization. The MW is kept low to maintain manageable viscosities in the low solvent formulation, thus allowing for continued use of existing equipment for application, with functional groups on the resin reacting on the vehicle surface to form the final coating product. The reduction in MW is achieved by higher initiator levels and polymerization temperatures (>120 °C) that result in several adventitious side reactions that have a marked effect on the final molecular weight and ultimately the end properties of the polymer. These reactions are accentuated under the starved-feed semibatch operating policy generally used to control copolymer composition and thus are believed to be the primary factor involved in the deviation from classical free radical polymerization rates.[1]

The secondary reactions of acrylates, an important component of many coatings resins, have been the focus of recent attention in the literature. It has been found that observed rates of polymerization[2,3] are significantly lower than would be expected from the chain-end propagation rate coefficient measured by pulsed laser polymerization.[4,5] This result is explained through an intramolecular chain transfer event followed by slow addition of monomer to the more stable tertiary radical, as shown in Scheme 1 for butyl acrylate (nBA). The propagating chain-end radical wraps around and abstracts a hydrogen atom from an acrylate unit on its own backbone via the formation of a six-membered ring. The resulting tertiary or midchain radical is believed to propagate at a much slower rate than the parent end-chain radical.

Scheme 1. Intramolecular Transfer to Polymer Followed by Monomer Addition to the Resulting Midchain Radical Structure To Create a Short-Chain Branch

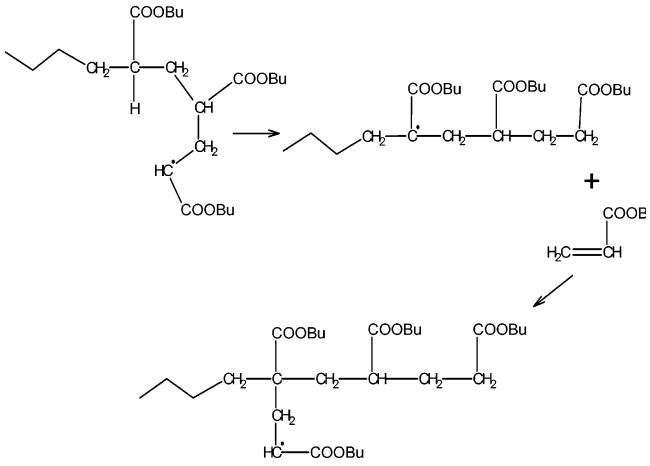

There is significant evidence supporting Scheme 1. The presence of the midchain radical has been directly observed via ESR.[6,7] Indirect evidence is based upon ^{13}C NMR measurement of the quaternary carbons in the polymer that result from addition to the midchain radical to form a short-chain branch, following the work of Ahmad et al.[8] The intramolecular chain transfer reaction, sometimes referred to as backbiting, is well-known in high-temperature ethylene homopolymerization, and it has been observed in ethylene/nBA copolymerization that the methine hydrogens on nBA units in the polymer chain are much more susceptible to abstraction than hydrogens from a CH_2 unit in the backbone.[9]

Formation of quaternary carbons can also occur via an intermolecular route whereby a hydrogen atom is abstracted from another polymer chain, as shown in Scheme 2. However, quaternary carbons are found under conditions of very low polymer concentration,[8,10] and an analysis of polymer gel fraction formed during nBA emulsion polymerization strongly suggests that the intramolecular (backbiting) mechanism is dominant.[3]

* Corresponding author: e-mail hutchra@chee.queensu.ca.

10.1021/ma049621t CCC: $27.50
Published on Web 07/17/2004

Scheme 2. Intermolecular Transfer to Polymer; Subsequent Monomer Addition Creates a Long-Chain Branch Point in the Polymer

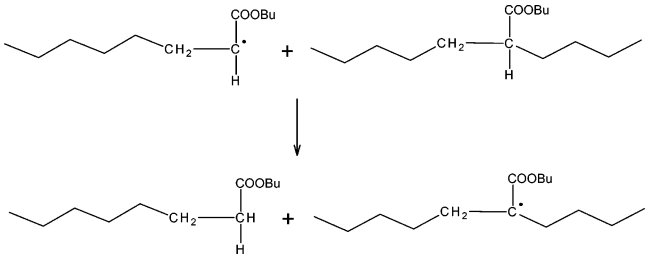

Scheme 3. β-Scission of nBA Midchain Radical

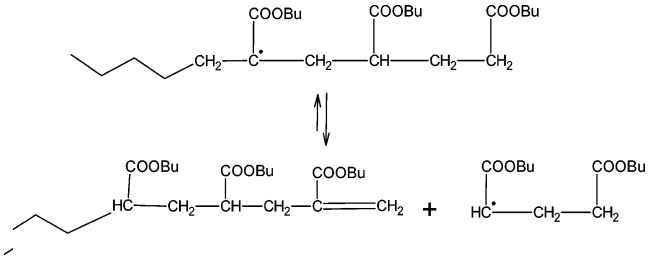

On the basis of this evidence, there is little doubt that the mechanisms shown in Scheme 1 must be considered when examining acrylate polymerization under the operating conditions used to produce acrylic resins for coatings. Indeed, they are believed to be important even under the low-temperature (20−30 °C) conditions at which nBA propagation kinetics have been studied by pulsed-laser polymerization.[11,12] The task, therefore, is to estimate the rate coefficients for the backbiting process (k_{bb}) and the addition of monomer to the midchain radical (k_p^{tert}).

An additional acrylate mechanism that must be considered under high-temperature polymerization conditions is the fragmentation or β-scission of the midchain radical (rate coefficient k_β) shown in Scheme 3. Chiefari and co-workers[13] first reported this process in poly(alkyl acrylates), measuring the concentration of unsaturated chain ends via proton NMR. At higher temperatures it was concluded that the majority of the chains in the system were terminated by β-scission. As shown in Scheme 3, the scission mechanism may be reversible; i.e., the unsaturated macromonomers are able to add to radicals in the system. However, under normal polymerization conditions the concentration of macromer chain ends remains low relative to monomer, and the reverse reaction can be neglected.

Although scission events can occur in any system where midchain radicals are formed, the mechanism has a higher activation energy than H-abstraction and thus becomes important only at elevated temperatures. The reaction is not believed to occur during butyl acrylate polymerization at 75 °C[3] but is shown to be important at 140 °C.[1,13] Electrospray ionization mass spectroscopy (ESI-MS) has been used to identify the unique chain-end structures formed by β-scission during acrylate polymerization under conditions typically used for production of coatings resins.[1] Hirano and Yamada[14] focused on the β-scission mechanism by examining the polymerization of the unsaturated trimer of methyl acrylate. By selecting this species, the authors were able to study competitive rates of β-scission and addition to the tertiary radical while eliminating the influence of secondary radicals. As done by Chiefari et al.,[13] ^{1}H NMR spectroscopy was used to detect the unsaturated end group (β-scission product) in the polymer. The estimated ratios of k_p^{tert}/k_β (L/mol) decreased from 7 at 50 °C to 0.9 at 130 °C. Although this result provides some idea of the relative rates of these competing reactions, it cannot be applied directly to acrylate polymerization since addition of monomer to the midchain radical should be faster than the corresponding addition of trimer due to reduced steric congestion, and propagation with trimer may also be affected by depropagation.[14]

The interplay of the branching and scission mechanisms is little understood. Busch and Müller[15] have developed a model of the system and applied it to the analysis of their higher temperature nBA polymerization results. The experimental results of Grady et al.[1] indicate that these mechanisms also occur at the conditions (∼140 °C, low monomer concentration) under which automotive coatings are produced. In this work, we examine a series of nBA starved feed semibatch polymerizations, varying monomer and polymer concentrations by manipulating monomer feed time and feed rate. The experimental results are used to estimate the unknown rate coefficients for the backbiting, addition to the tertiary radical, and β-scission mechanisms. A mechanistic model including these additional reactions has been formulated using the Predici software package,[16] and a comparison of simulation and experiment provides some additional insight into this complex system.

Table 1. Experimental Conditions for Semibatch nBA Polymerizations[a]

feed time (min)[b]	final wt % nBA	nBA feed (g)	TBPA feed (g)	xylene feed (g)	nBA feed rate (g/min)
90	20	150	2.10	390	1.7
90	50	350	4.88	150	3.9
90	80	800	11.25	0	8.9
180	20	160	2.25	405	0.9
180	38	360	5.03	405	2.0
180	53	440	6.15	200	2.4
180	80	800	11.18	0	4.4
360	20	150	2.10	390	0.4
360	50	350	4.88	150	1.0
360	80	800	11.25	0	2.2

[a] Initial solvent charge of 194 g, T = 138 °C, and 0.014 g of TBPA/g of nBA for all cases. [b] Monomer feed time. The initiator and solvent are fed over a longer time period (monomer feed time + 15 min).

Experimental Section

The polymerizations were carried out following procedures similar to those used to produce coatings resins industrially.[1] All reagents were obtained from Sigma-Aldrich and used as received. The nBA monomer contained 10−55 ppm 4-methoxyphenol inhibitor, xylene solvent was an isomeric mix with an atmospheric boiling point range of 137−140 °C, and *tert*-butyl peroxyacetate (TBPA) initiator, obtained as a 75 wt % solution in mineral spirits, was stored under 10 °C.

All semibatch polymerizations were carried out in a Mettler/Toledo Lab Max reactor system consisting of a 1 L glass vessel with a dual blade agitator and reflux condenser. 194 g of xylene solvent was heated to 138 °C under a N_2 blanket, followed by the feeding of nBA and initiator/solvent mixture at fixed mass flow rates over fixed time intervals, as summarized in Table 1. The process was controlled using a Camile control and data acquisition system with automatic feed and temperature control. Samples were collected into an inhibited xylene solution at regular intervals and cooled in an ice bath.

Monomer concentrations in diluted samples were measured using a Varian CP-3800 gas chromatograph consisting of a CP8771 WCOT fused silica column of length 30 m and i.d. of

0.25 mm and a flame ionization detector. The carrier gases were ultrahigh-purity N_2 and He held under a constant pressure of 16.2 psi, and the combustion gases were ultrahigh-purity H_2 and zero grade compressed air. Concentrations were determined relative to a series of calibration standards.

The molecular weights and polydispersities of all samples were determined using a size exclusion chromatograph (SEC) consisting of a Waters 2960 separation module connected to a Waters 410 differential refractometer. The molecular weight data of the poly(acrylate) samples are reported relative to polystyrene. Calculations using published Mark−Houwink calibration parameters[4] indicate that this assumption introduces, at most, an error of 5%. In addition, previous work using ESI-MS has shown that there is no significant difference in elution times for pBA and pS samples of low MW (<10 000),[1] and this has been confirmed more recently by measurements using SEC with a light scattering detector.[17] Thus, the MW values can be regarded as absolute. The calibration curve was constructed using 10 narrow polydispersity polystyrene standards. Calculated polydispersities were lower than expected for some pBA samples (<1.5). While a possible indication that acrylate branching could be affecting elution behavior of the polymer, low polydispersities have also been reported for methacrylate (and thus nonbranched) coatings resins[18] and may result from other experimental artifacts such as loss of low-MW material during polymer isolation prior to SEC analysis.

Replicated runs, repeat measurements on [nBA] and MWs, and a check of the total nBA content (free monomer + polymer, with polymer content measured by gravimetry) provide a high level of confidence in the experimental data. Further details are found in ref 19.

All poly(*n*-butyl acrylate) NMR samples were analyzed using either a 400 MHz Bruker Avance instrument or a 500 MHz Bruker Avance (DRX) instrument. The samples were prepared by dissolving dry polymer in deuterated chloroform ($CDCl_3$) to approximately 20% w/w. All peaks in the ^1H spectrum were integrated with respect to the O−CH_2 group of the alkyl chain, the macromer peaks of interest being those at 5.56 and 6.15 ppm.[13,20] The values, reported per 100 nBA repeat units in the polymer, were estimated by summing the integrals of these two peaks and dividing by two. Peaks in the ^{13}C spectrum were integrated with respect to the large O−CH_2−CH_2−CH_2−CH_3 resonance at 13.9 ppm. The level of branching was calculated by integrating the quaternary carbon peak at 47.9−48.8 ppm[2,8,20] and is reported on the basis of 100 repeat units contained in the polymer.

Mechanistic Model of nBA Polymerization

A model has been constructed in Predici to more effectively analyze the high-temperature, free radical polymerization of nBA. The base model includes initiation, propagation, termination, transfer to monomer and solvent (Scheme 4), and their associated kinetic expressions. The subscript *n* denotes the number of monomeric units in growing polymer radicals (P_n) and dead polymer chains (D_n). The free radical initiator (I) unimolecularly decomposes with rate coefficient k_d to form two primary radicals (I*) with efficiency *f*. Chain initiation occurs when the primary radical adds to monomer M, and chain growth continues via successive addition of monomer units to the radical center (chain propagation, with rate coefficient k_p). Bimolecular coupling of two growing chains results in the loss of two radicals in the system and the formation of either one (termination by combination) or two (termination by disproportionation) dead polymer chains. The amount of disproportionation is described by α, the fraction of the total termination rate coefficient k_t (combination + disproportionation). Chain stoppage may also occur via a transfer mechanism, where the growing radical abstracts a weakly bonded atom (usually hydrogen) from monomer or solvent (denoted by S) to generate a dead polymer chain as well as a new radical that initiates another polymer chain. The reactions in Scheme 4 can be referred to collectively as the classical model.

Scheme 4. Base Mechanistic Set for nBA Free Radical Polymerization

$$\mathrm{I} \xrightarrow{k_d} 2f\,I^{\bullet}$$

$$I^{\bullet} + M \xrightarrow{k_p} P_1$$

$$P_n + M \xrightarrow{k_p} P_{n+1}$$

$$P_n + P_m \xrightarrow{(1-\alpha)k_t} D_{n+m}$$

$$P_n + P_m \xrightarrow{\alpha k_t} D_n + D_m$$

$$P_n + M \xrightarrow{k_{tr}^{mon}} D_n + P_1$$

$$P_n + S \xrightarrow{k_{tr}^{sol}} D_n + P_1$$

Scheme 5. Additional nBA Mechanisms Involving Formation (by Intramolecular Transfer) and Reaction of Midchain Radical

$$P_n \xrightarrow{k_{bb}} Q_n$$

$$Q_n + M \xrightarrow{k_p^{tert}} P_{n+1} + SCB$$

$$Q_n \xrightarrow{k_\beta} D^{=}_{n-2} + P_2$$

$$Q_n + P_m \xrightarrow{(1-\alpha_{pq})k_t} D_{n+m}$$

$$Q_n + P_m \xrightarrow{\alpha_{pq}k_t} D_n + D_m$$

$$Q_n + Q_m \xrightarrow{(1-\alpha_{qq})k_t^{tert}} D_{n+m}$$

$$Q_n + Q_m \xrightarrow{\alpha_{qq}k_t^{tert}} D_n + \mathrm{D_m}$$

The extended model includes the additional mechanisms of intramolecular H atom abstraction, monomer addition, β-scission, and termination of the resulting tertiary radical, as shown in Scheme 5. The propagating chain-end radical undergoes the backbiting abstraction process to form a tertiary radical species, Q_n, with the associated rate constant of k_{bb}. This structure is able to undergo monomer addition to form a short-chain branch (SCB) in the polymer. The addition of monomer to the midchain radical is much slower than to the radical chain end: thus, k_p^{tert} is expressed as a fraction γ of the chain-end propagation coefficient ($k_p^{tert} = \gamma k_p$). After the first monomer addition, the propagating radical assumes secondary chain end character and continues growth with the normal k_p value. The β-scission reaction is implemented in an irreversible form (rate coefficient k_β), with the tertiary radical fragmenting to form the long chain unsaturated (as indicated by the "=" subscript) dead polymer species and a short-chain radical of length two. This integer value is a reasonable approximation of the actual radical structure formed by β-scission that, as seen in Scheme 3, is a CH_2 group short of a true dimeric radical. Note that β-scission to form an unsaturated trimer species and a long chain

Table 2. Kinetic Coefficients for High-Temperature (138 °C) Free Radical Polymerization of nBA in Xylene Solvent with TBPA Initiator

coeff	freq factor	activ energy (kJ/mol)	value at 138 °C	reference
k_d (s^{-1})	6.78×10^{15}	147.2	1.14×10^{-3}	23
f			0.5	1
k_p (L/(mol s))	1.80×10^{7}	17.4	1.16×10^{5}	4
k_t (L/(mol s))	2.57×10^{8}	2.4	1.26×10^{8}	21
α			0.1	
k_{tr}^{mon}/k_p	1.60×10^{-2}	15.2	1.87×10^{-4}	24
k_{tr}^{sol}/k_p	1.76×10^{1}	32.2	1.43×10^{-3}	25
α_{pq}			0.7	
α_{qq}			0.9	
k_{bb} (s^{-1})			4000	this work
$\gamma = k_p^{tert}/k_p$			0.0012	this work
k_β (s^{-1})			6	this work

radical of length ($n - 2$) is not considered in the model. While the possibility of this reaction cannot be completely ruled out, no trace of the short-chain unsaturated species could be found by ESI-MS.

The tertiary radical can also undergo termination by disproportionation or combination with either a chain-end or another tertiary radical. Although a recent study[14] suggests that the coefficient for Q−Q termination (k_t^{tert}) may be more than an order of magnitude lower than chain-end termination (k_t), the k_t value taken from the literature[21] was estimated from experimental data without accounting for the presence of midchain radicals and thus can be considered an averaged value for the nBA system. For this reason we assume that the termination rate coefficient is independent of radical type, such that $k_t^{tert} = k_t$. However, the fraction of termination by disproportionation (α, α_{pq}, α_{qq}) is varied depending on whether termination involves radical types P−P, P−Q, or Q−Q since tertiary carbon radicals are more likely to undergo disproportionation than secondary radicals.[22]

The values for the rate coefficients associated with Schemes 4 and 5 are summarized in Table 2. Values for k_d,[23] k_p,[4] k_t,[21] and k_{tr}^{mon} [24] are taken from recent literature as measured using specialized kinetic techniques. The estimate for transfer to solvent is based upon an older study of ethyl acrylate/toluene,[25] with the preexponential value decreased by 10% in order to improve the fit of the model to MW data. Values for α, the fraction of termination by disproportionation, were set under the assumption that the majority of P−P termination is by combination and the majority of Q−Q termination is by disproportionation, with the level of disproportionation for P−Q termination intermediate between the two.[22]

There are three unknown rate coefficients that must be estimated for intramolecular hydrogen transfer (k_{bb}), the propagation of the tertiary radical ($k_p^{tert} = \gamma k_p$), and the rate of β-scission (k_β). Experimental data for the additional mechanisms considered in this work are scarce. The estimates in Table 2 were obtained by fitting of NMR and rate data, as discussed later.

Results and Discussion

Figure 1 shows the nBA concentration and polymer number-average MW (M_n) profiles for reactions with a final polymer content of 20, 50, and 80 wt % in xylene solution and a monomer feed time of 180 min. The results are typical of starved feed semibatch operation. Monomer concentrations are low at all times, settling to a level of 0.2−0.4 mol/L for the last two-thirds of the

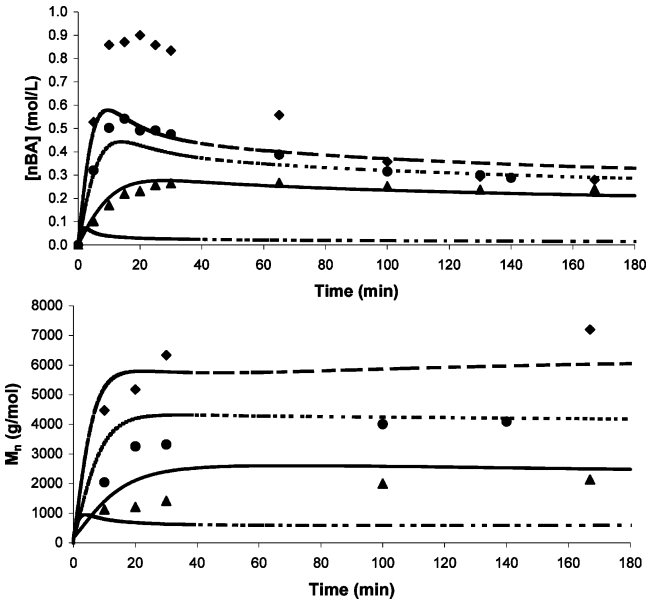

Figure 1. Monomer concentration (top) and number-average molecular weight (bottom) profiles for 180 min nBA semibatch polymerizations. Points indicate experimental values and lines simulation results with final polymer content of 20% (▲,—), 50% (●, - - -), and 80% (◆, — —) in xylene solution. Additional line (-- — --) indicates the simulation results using the classical model for the 50% case.

3 h experiment. The shape of the initial transient period is dependent on the monomer addition rate, with higher levels of unreacted monomer evident for the reactions with higher feed rates. The MW averages also quickly plateau, with higher M_n values obtained for the experiments with higher rates of monomer addition: 7000 g/mol for a final polymer content of 80% and only 2000 g/mol for the experiment with a final polymer level of 20%. In addition to simulation results from the full model discussed later, the predictions obtained using only the classical kinetic mechanisms of Scheme 4 are shown for the experiment with a final polymer level of 50%. Neglecting the formation of midchain radicals and their low reactivity leads to an overprediction of reaction rate (low predicted levels of [nBA]), as also observed by Plessis et al.[2,3]

The variation of feed times and final nBA levels for the complete set of experiments (see Table 1) is much larger than that presented by Grady et al.[1] and provides additional detail into the controlling mechanisms under industrial conditions. In addition, the experimentally determined levels of branch points and macromer ends provide a more direct means of estimating the unknown rate coefficients. From the mechanisms in Scheme 5, the following rate expressions may be written, where [P] is the total chain-end radical concentration and [Q] is the total tertiary radical concentration:

$$R_{bb} = k_{bb}[P] \quad (1)$$

$$R_{beta} = k_\beta[Q] \quad (2)$$

$$R_{scb} = \gamma k_p[M][Q] \quad (3)$$

$$R_t^Q = k_t[Q]([Q] + [P]) \quad (4)$$

R_{beta} is the rate of beta scission, R_{bb} the rate of polymer backbiting, R_{scb} the rate of short-chain branching (the

rate of addition to the tertiary radical), and R_t^Q the rate of termination of the tertiary radical formed after backbiting.

Assuming steady state on the tertiary radical species, the rates can be equated:

$$R_{bb} = R_{beta} + R_{scb} + R_t^Q \quad (5)$$

If the rate of termination of the tertiary radical is significantly less than that of β-scission or short-chain branching, the ratio of the tertiary radical concentration to the chain end radical concentration can be written as

$$\frac{[Q]}{[P]} = \frac{k_{bb}}{\gamma k_p[M] + k_\beta} \quad (6)$$

Since almost all of the branch points present in the polymer are attributed to short-chain branching,[3] the ^{13}C NMR measure of quaternary carbons ratioed to the total number of repeat units (r.u.) can be expressed as

$$[SCB]_{NMR} = \frac{\text{no. of } C_4}{\text{no. of r.u.}} = \frac{R_{scb}}{R_p + R_{scb}} = \frac{\gamma k_p[Q]}{k_p[P] + \gamma k_p[Q]} \quad (7)$$

Since the reactivity of the tertiary radical is much less than that of the secondary propagation radical ($k_p[P] \gg \gamma k_p[Q]$)

$$[SCB]_{NMR} = \frac{\gamma[Q]}{[P]} = \frac{k_p^{tert}[Q]}{k_p[P]} \quad (8)$$

A similar ratio can be derived for the ^1H NMR spectroscopic measure of the concentration of unsaturated chain ends, or macromer groups, in the polymer. If these unsaturated end groups are formed primarily by β-scission[13] and do not react further, the ratio for the total number of macromer end groups to the total number of repeat units can be written as

$$[MAC]_{NMR} = \frac{\text{no. of macromers}}{\text{no. of r.u.}} = \frac{R_{beta}}{R_p + R_{scb}} = \frac{k_\beta[Q]}{k_p[P][M]} \quad (9)$$

Neglecting the consumption of tertiary radicals by termination,[26] the sum of branching and scission events is equal to the frequency of backbiting events. Thus

$$\frac{R_{bb}}{R_p} = \frac{R_{beta} + R_{scb}}{R_p} = \frac{k_{bb}[P]}{k_p[M][P]} = \frac{k_{bb}}{k_p[M]} \quad (10)$$

and k_{bb} can be estimated from the sum of macromer and quaternary carbon units measured by NMR:

$$k_{bb} = ([SCB]_{NMR} + [MAC]_{NMR})k_p[M] \quad (11)$$

The ratio of quaternary carbon to macromer units provides a measure of the relative significance of addition to and β-scission of the tertiary radical:

$$\frac{R_{scb}}{R_{beta}} = \frac{\gamma k_p[M][Q]}{k_\beta[Q]} = \frac{\gamma k_p}{k_\beta}[M] = \frac{[SCB]_{NMR}}{[MAC]_{NMR}} \quad (12)$$

Table 3. Final Butyl Acrylate Concentration ($[nBA]_f$), SCB and Macromer Levels Measured by NMR, and Estimated Kinetic Coefficients for Reactions Involving Midchain Radicals

feed time (min)	final wt % polymer	$[nBA]_f$ (mol/L)	[SCB][a]	[MAC][a]	k_{bb} (s^{-1})	$\gamma k_p/k_\beta$ (L/mol)
90	20	0.28	8.66	1.50	3380	20.6
	50	0.34	8.76	0.60	3780	42.9
	80	0.35	7.80	0.35	3390	63.7
180	20	0.24	8.90	1.45	2950	25.6
	50	0.29	10.57	0.65	3860	56.1
	80	0.31	9.13	0.45	3520	65.4
360	20	0.19	8.57	1.50	2270	30.1
	50	0.24	9.91	0.65	3010	63.5
	80	0.30	9.23	0.50	3460	61.5

[a] Per 100 monomer repeat units in the polymer.

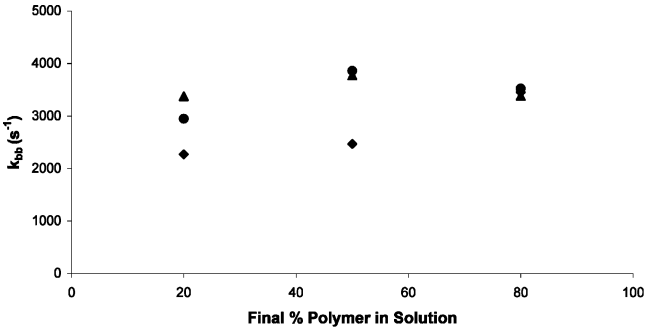

Figure 2. k_{bb} (s^{-1}) estimates from NMR analysis for nBA polymerization at 138 °C plotted against final polymer content for feed times of (▲) 90, (●) 180 and (◆) 360 min.

If this ratio is large, then monomer addition and branch formation is favored. Thus, NMR provides a relatively direct means of estimating some of the unknown rate coefficients in the system. It should be emphasized that the simplifications and assumptions used to derive eqs 11 and 12 for analysis of NMR data are not made in the mechanistic model implemented in Predici.

Table 3 contains the results from the NMR analysis of the polymer samples taken at the end of each experiment. The samples have a high level of branching, with 8−10 quaternary carbons measured per 100 repeat units. The observation that this value is not a function of final wt % polymer in the reactor validates previous work,[3,8] concluding that the branch points are formed mainly by intramolecular transfer events. The macromer level is significantly lower, in the range of 0.5−1.5 per 100 repeat units. This latter value can be coupled with average chain length to calculate that between 20 and 35% of chains in the system are macromer-terminated. This result is in contrast with those of Chiefari et al.,[13] in which close to 100% of the chains produced were macromers. The difference can be explained by the much higher radical concentrations in our experiments and the corresponding higher rates of termination producing saturated chain-end structures. Since monomer and radical concentrations remain relatively constant over the course of the semibatch reaction, the NMR measurements are combined with the [nBA] level at the end of the experiment to estimate k_{bb} and $\gamma k_p/k_\beta$ using eqs 11 and 12. These estimates are also included in Table 3 and plotted against final polymer level in Figures 2 and 3.

Figure 2 shows a substantial amount of variability for k_{bb} calculated from the data, with estimates between 2200 and 3900 s^{-1}. However, no variation with the final nBA level (wt % polymer) or feed time can be seen

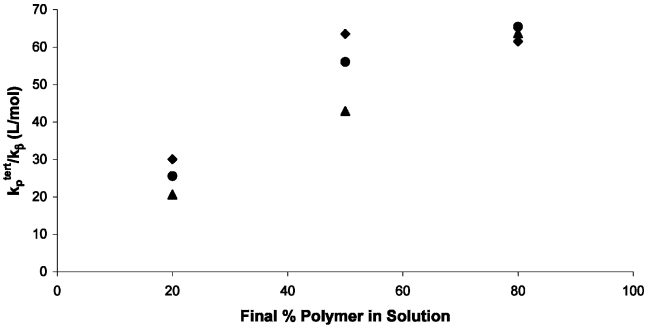

Figure 3. $\gamma k_p/k_\beta$ (L/mol) estimates from NMR analysis for nBA polymerizations at 138 °C plotted against final polymer content for feed times of (▲) 90, (●) 180, and (◆) 360 min.

within the scatter of the data. A value of 4000 s^{-1} is used for the simulations presented later in this section.[26] The estimates for $\gamma k_p/k_\beta$ ($= k_p^{tert}/k_\beta$) plotted in Figure 3 also show significant scatter, some of which can be attributed to taking the ratio of two experimental NMR values. It is clear, however, that monomer addition to the tertiary radicals is favored over β-scission. The ratio shows an unexpected variation with final polymer content in the reactor, increasing from 20 to 30 L/mol at 20 wt % polymer to 60 to 65 L/mol at 80%. This trend indicates that the assumptions used to derive the relationship between the ratio and the NMR data are not entirely valid. Nonetheless, the data provide a crude estimate for the ratio of the two unknown coefficients, k_p^{tert} and k_β. γ ($= k_p^{tert}/k_p$) was adjusted to the value of 1.2×10^{-3} to provide a reasonable representation of [nBA] levels in the series of experiments, and k_β was fixed at 6 s^{-1}. The absolute value of k_p^{tert} is thus 140 L/(mol s), a value intermediate between the addition rate of acrylate trimer to a midchain acrylate radical[14] and the addition rate of acrylate monomer to a tertiary methacrylate chain-end radical.[17] The resulting k_p^{tert}/k_β ratio of 24 is higher than that reported by Hirano and Yamada,[14] suggesting that monomer adds to the tertiary radical at a significantly faster rate than trimer.

Using these estimates for the additional rate coefficients, it must be examined whether the extended model provides a reasonable representation of the data set over the wide range of conditions explored experimentally. The simulated [nBA] profiles against data for the 180 min semibatch experiments are shown in Figure 1. The model provides a good representation of the experimental data, with the exception of the first hour of the experiment with the highest monomer feed rate (final polymer content of 80 wt %). The reason for this mismatch, also observed for the 80% 90 and 360 min experiments, is under further investigation. A comparison of model predictions against the complete set of experimental data is provided in Figure 4, which plots the final [nBA] value (measured at the end of the semibatch feeding time) against the final polymer level. The model predictions fit the experimental free monomer data quite well, quantitatively capturing the increase in [nBA] observed with increasing final polymer level and with decreasing monomer feed time.

As shown in Figure 1, the model provides a good representation of the relatively constant M_n values vs time as well as the increase in M_n observed with final polymer level. It is interesting to note that the classical model predicts a very low molecular weight with respect to the extended model which includes an additional

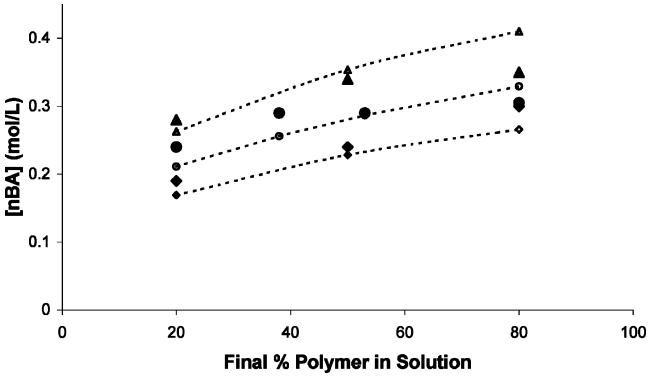

Figure 4. Monomer concentration at end of feed time vs final polymer content. Closed symbols indicate experimental values and open symbols simulation predictions for feed times of (▲) 90, (●) 180, and (◆) 360 min. Dashed lines connecting simulation results are drawn as a guide to the eye.

chain stopping mechanism (β-scission) and a slow propagation step. This can be understood by examining the expression for instantaneous chain length, written as

$$DP_n^{inst} = \frac{(k_p[P] + \gamma k_p[Q])[M]}{(k_{td} + 0.5k_{tc})([P] + [Q])^2 + k_{tr}^{mon}[M][P] + k_{tr}^{sol}[S][P] + k_\beta[Q]} \quad (13)$$

Adding the extra reactions significantly decreases [P] while increasing [M], affecting both the propagation and transfer terms and having a smaller effect on overall rate of termination. The complex balance of terms leads to a predicted increase in chain length for the extended model compared to the classical model.

Figure 5 plots the molecular weight averages measured at the end of the semibatch feeding time against the final polymer loading. MW averages increase with increasing final polymer level and with decreasing monomer feed time. The model captures these trends but is unable to predict the sharp increase observed at 80 wt % polymer. A possible explanation for the observed increase is that long-chain branching (as depicted in Scheme 2 or as initiated by backbone H atom abstraction by a primary initiator radical) can cause a significant increase in M_w. As seen in Figure 6, the experimental polydispersity increases significantly with polymer content, a clear indication of long-chain branching. The model, which does not include this mechanism, predicts polydispersity between 2 and 2.5 and does not capture the behavior observed experimentally. The observed increase in M_n with polymer content is more difficult to explain. It may result from the reactivity of the unsaturated (macromer) end groups, another mechanism not considered in the model. However, the experimental MWDs show no sign of the bimodality observed elsewhere when macromers react and are incorporated into other growing chains.[27]

Figure 7 plots the experimental values and model predictions for quaternary carbons and macromer end groups of the final polymer samples. The macromer level is predicted to decrease with increasing polymer content in the reactor, as observed experimentally. However, the model predicts that the monomer feed time should also have a significant effect on macromer content, a trend not observed experimentally. Similarly, while the model

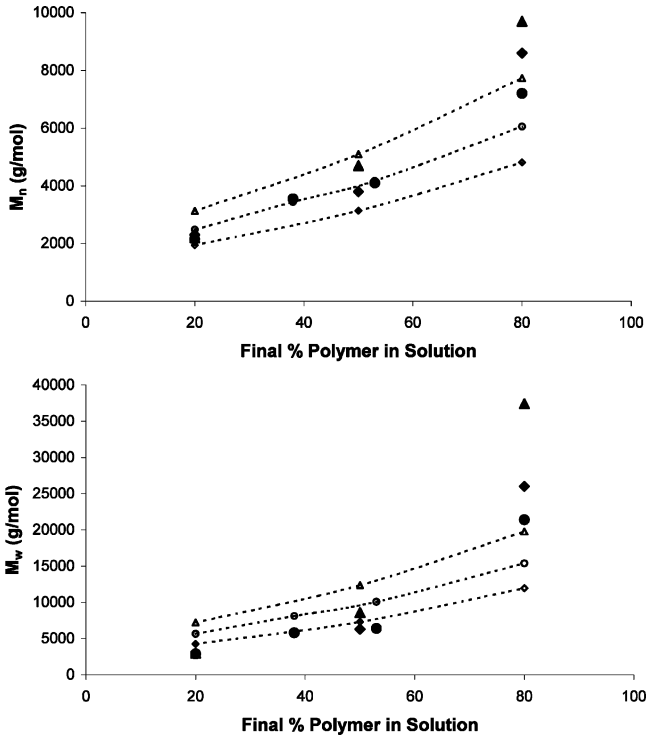

Figure 5. Final M_n (top) and M_w (bottom) values at end of monomer feed vs final polymer content. Closed symbols indicate experimental values and open symbols simulation predictions for feed times of (▲) 90, (●) 180, and (◆) 360 min. Dashed lines connecting simulation results are drawn as a guide to the eye.

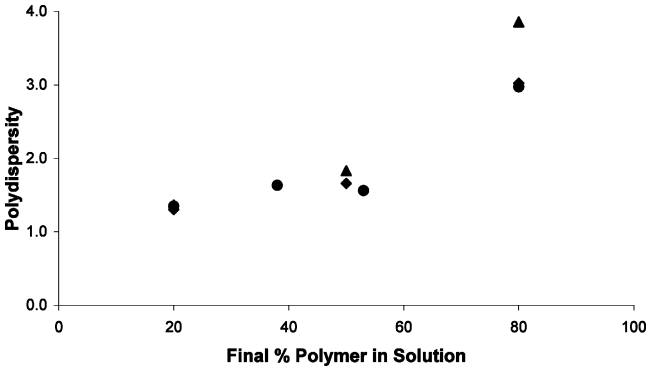

Figure 6. Experimental polydispersities plotted against final polymer concentration. Symbols indicate experiments with monomer feed times of (▲) 90, (●) 180, and (◆) 360 min.

predicts the general level of quaternary carbons observed experimentally, it is not able to quantitatively match the observed values over the entire experimental space, indicating that the set of mechanisms in the model is still not complete. The effect of reduced termination rates for midchain radicals[14] will be examined via simulation, as will the effect of macromer reactivity, as recent work indicates that macromer is as reactive as monomer toward radicals.[27,28] This latter mechanism is expected to have only a minor effect, however, as the concentration of macromer is more than an order of magnitude lower than that of monomer in the starved-feed system, even at the end of the batch.

Conclusions

A mechanistic model of the high-temperature polymerization of nBA has been formulated that includes the important secondary reactions of backbiting and monomer addition to and β-scission of the resulting tertiary radical. Rate coefficients for these processes are estimated using NMR and rate data for a series of semibatch solution polymerizations carried out over a wide range of polymer levels and monomer feed rates. Backbiting is demonstrated to be a dominant reaction, with subsequent monomer addition leading to 8−10 quaternary carbons per 100 nBA repeat units in the polymer. β-Scission, although occurring less frequently, has an important effect on polymer MW.

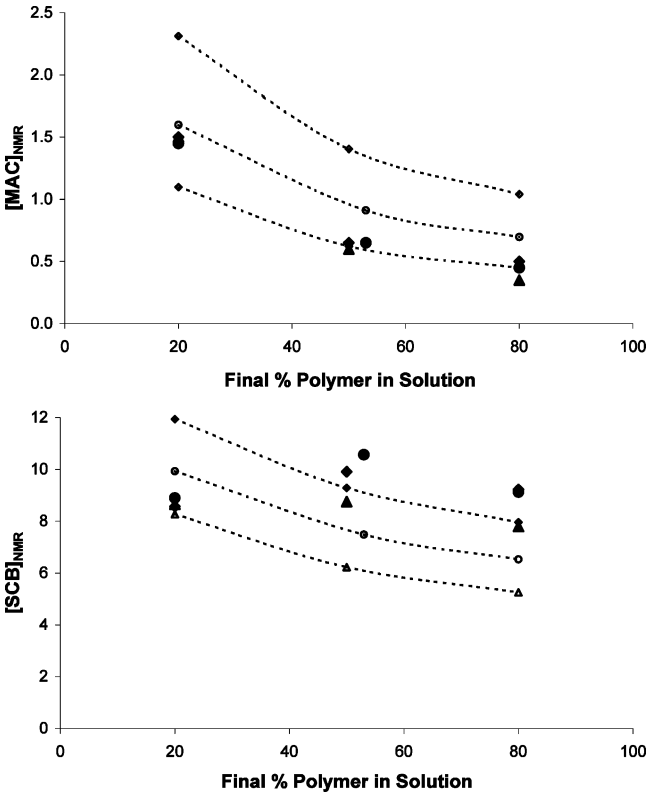

Figure 7. Final macromer (top) and quaternary carbon (bottom) levels per 100 monomeric repeat units at end of monomer feed vs final polymer content. Closed symbols indicate experimental values and open symbols simulation predictions for feed times of (▲) 90, (●) 180, and (◆) 360 min. Dashed lines connecting simulation results are drawn as a guide to the eye.

The model developed provides a reasonable representation of how experimental free monomer levels, polymer MWs, and NMR-measured quaternary carbons and macromer end groups vary with monomer feed rate and final polymer level. While providing a dramatic improvement over predictions of a classical polymerization model, some small systematic variations suggest that further improvements are possible. MW deviations observed at high polymer concentrations indicate that intermolecular H-abstraction should be added to the model. The importance of macromer reactivity and reduced termination of the tertiary radicals will also be examined in future work. The improved representation of acrylate polymerization is also being used in modeling of acrylate/methacrylate copolymerization.[17]

Acknowledgment. We thank E. I. du Pont de Nemours and Co., the Centre for Automotive Materials and Manufacturing, and the Natural Sciences and Engineering Research Council of Canada for financial support, Michael Grady (DuPont) for helpful technical

discussions, and Joan Hansen and Michele Bednarek (DuPont) for NMR analysis.

References and Notes

(1) Grady, M. C.; Simonsick, W. J.; Hutchinson, R. A. *Macromol. Symp.* **2002**, *182*, 149−168.
(2) Plessis, C.; Arzamendi, G.; Leiza, J. R.; Schoonbrood, H. A. S.; Charmot, D.; Asua, J. M. *Macromolecules* **2000**, *33*, 4−7.
(3) Plessis, C.; Arzamendi, G.; Leiza, J. R.; Schoonbrood, H. A. S.; Charmot, D.; Asua, J. M. *Ind. Eng. Chem. Res.* **2001**, *40*, 3883−3894.
(4) Beuermann, S.; Paquet, D. A., Jr.; McMinn, J. H.; Hutchinson, R. A. *Macromolecules* **1996**, *29*, 4206−4215.
(5) Lyons, R. A.; Hutovic, J.; Piton, M. C.; Christie, D. I.; Clay, P. A.; Manders, B. G.; Kable, S. H.; Gilbert, R. G. *Macromolecules* **1996**, *29*, 1918−1927.
(6) Gilbert, B. C.; Lindsay Smith, J. R.; Milne, E. C.; Whitwood, A. C.; Taylor, P. *J. Chem. Soc., Perkin Trans.* **1994**, *2*, 1759−1769.
(7) Yamada, B.; Azukizawa, M.; Yamazoe, H.; Hill, D.; Pomery, P. J. *Polymer* **2000**, *41*, 5611−5618.
(8) Ahmad, N. M.; Heatley, F.; Lovell, P. A. *Macromolecules* **1998**, *31*, 2822−2827.
(9) McCord, E. F.; Shaw, W. H., Jr.; Hutchinson, R. A. *Macromolecules* **1997**, *30*, 246−256.
(10) Plessis, C.; Arzamendi, G.; Alberdi, J. M.; van Herk, A. M.; Leiza, J. R.; Asua, J. M. *Macromol. Rapid Commun.* **2003**, *24*, 173−177.
(11) Nikitin, A. N.; Castignolles, P.; Charleux, B.; Vairon, J.-P. *Macromol. Theory Simul.* **2003**, *12*, 440−448.
(12) Arzamendi, G.; Plessis, C.; Leiza, J. R.; Asua, J. M. *Macromol. Theory Simul.* **2003**, *12*, 315−324.
(13) Chiefari, J.; Jeffery, J.; Mayadunne, R. T. A.; Moad, G.; Rizzardo, E.; Thang, S. N. *Macromolecules* **1999**, *32*, 7700−7702.
(14) Hirano, T.; Yamada, B. *Polymer* **2003**, *44*, 347−354.
(15) Busch, M.; Müller, M. *Macromol. Symp.* **2004**, *206*, 399−418.
(16) Wulkow, M. *Macromol. Theory Simul.* **1996**, *5*, 393−416.
(17) Li, D.; Grady, M. C.; Hutchinson, R. A. Submitted for publication. Li, D. MSc Thesis, Queen's University, Kingston, ON, 2003.
(18) Beuermann, S.; Buback, M.; Jürgens, M. *Ind. Eng. Chem. Res.* **2003**, *42*, 6338−6342.
(19) Peck, A. F. N. MSc Thesis, Queen's University, Kingston, ON, 2003.
(20) Quan, C.; Soroush, M.; Grady, M. C.; Hansen, J. E. Submitted for publication.
(21) Beuermann, S.; Buback, M. *Prog. Polym. Sci.* **2002**, *27*, 191−254.
(22) Moad, G.; Solomon, D. H. *The Chemistry of Free Radical Polymerization*; Elsevier Science Inc.: Tarrytown, NY, 1995.
(23) Buback, M.; Klingbeil, S.; Sandmann, J.; Sderra, M.-B.; Vögele, H. P.; Wackerbarth, H.; Wittkowski, L. *Z. Phys. Chem.* **1999**, *210*, 199−221.
(24) Maeder, S.; Gilbert, R. G. *Macromolecules* **1998**, *31*, 4410−4418.
(25) Raghuram, P. V. T.; Nandi, U. S. *J. Polym. Sci., Part A-1* **1970**, *8*, 3079−3088.
(26) Neglecting termination of the tertiary radical in this analysis provides a lower bound for the estimates of k_{bb} from NMR data; thus, the model value of 4000 s^{-1} is slightly higher than the range of data in Table 3.
(27) Yamada, B.; Oku, F.; Harada, T. *J. Polym. Sci., Part A: Polym. Chem.* **2003**, *41*, 645−654.
(28) Harada, T.; Zetterlund, P. B.; Yamada, B. *J. Polym. Sci., Part A: Polym. Chem.* **2004**, *42*, 597−607.

MA049621T